AD-A166 615 A COMPREHENSIVE ANALYSIS ALGORITHM FOR ABLATION 1/1
TEMPERATURE FIELDS AND TH..(U) FOREIGN TECHNOLOGY DIV
WRIGHT-PATTERSON AFB OH 24 FEB 86 FTD-ID(RS)T-0746-85
UNCLASSIFIED F/G 22/2 NL

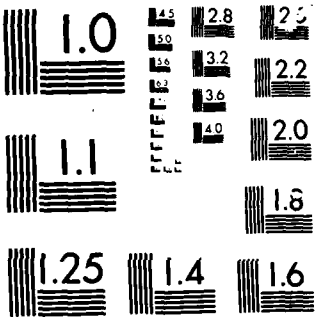


MICROCOP CHART

FTD-ID(RS)T-0746-85

# FOREIGN TECHNOLOGY DIVISION


## A COMPREHENSIVE ANALYSIS ALGORITHM FOR ABLATION, TEMPERATURE FIELDS AND THERMAL STRESSES OF THE CARBON-BASE NOSETIPS

by

Zhen zhong Huang

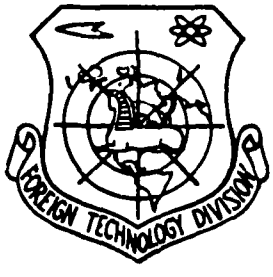






Approved for public release;
distribution unlimited.

# DISCLAIMER NOTICE

THIS DOCUMENT IS BEST QUALITY PRACTICABLE. THE COPY FURNISHED TO DTIC CONTAINED A SIGNIFICANT NUMBER OF PAGES WHICH DO NOT REPRODUCE LEGIBLY.

# EDITED TRANSLATION

FTD-ID(RS)T-0746-85 24 Feb 86

MICROFICHE NR: FTD-86-C-001528

A COMPREHENSIVE ANALYSIS ALGORITHM FOR ABLATION, TEMPERATURE FIELDS AND THERMAL STRESSES OF THE CARBON-BASE NOSETIPS

By: Zhen zhong Huang

English pages: 20

Source: Yuhang Xuebao, Nr. 7, 1984, pp. 30-38

Country of origin: China
Translated by: SCITRAN
F33657-84-D-0165
Requester: FTD/TQTA




PREPARED BY:

TRANSLATION DIVISION
FOREIGN TECHNOLOGY DIVISION
WP-AFB, OHIO.

GRAPHICS DISCLAIMER

All figures, graphics, tables, equations, etc. merged into this translation were extracted from the best quality copy available.

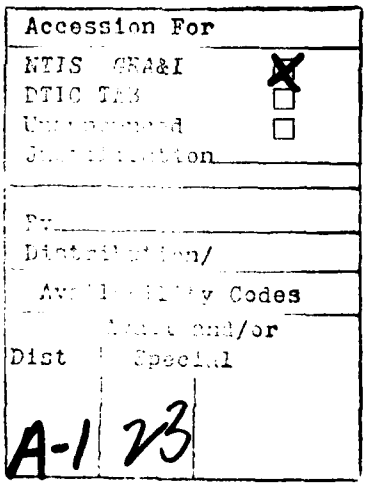

# A COMPREHENSIVE ANALYSIS ALGORITHM FOR ABLATION, TEMPERATURE FIELDS AND THERMAL STRESSES OF THE CARBON-BASE NOSETIPS

Zhen zhong Huang

## ABSTRACT

In this paper, the principles of the synthetic analysis and treatment techniques concerning vehicle re-entry thermal environment, ablation, heat transfer and thermal stresses are described. The thermochemical ablation calculations for chemical reactions on the ablating surfaces of carbon-base materials are simplified using selective calculation results. The temperature fields are calculated using the three-level explicit difference schemes for both constant and non-constant space steps within the total region. The thermal stresses are calculated, based on the incomplete generalized potential energy variational principles under the supposed conditions of linear elasticity, using the finite element method. This method can also be used to calculate the effects of the various displacement boundary conditions. An automatic grid generation technique has been developed during the computer code editing, which helps improve the shape selection calculations.

Received November 12, 1982.

## NOMENCLATURE

$A(e_{ij})$ = specific strain energy

$B$ = dimensionless rate of ablation

$c$ = specific heat

$c_\theta = (\partial r/\partial\theta)_\phi$

$c_\phi = (\partial r/r \sin\theta\partial\phi)_\theta$

$e_{ij}$ = strain tensor

$f_c^{(i)}$ = the rate of carbon ablation of the ith chemical reaction to total rate of ablation in chemical burning

$F_i$ = body force

$h$ = enthalpy

$H$ = height

$h_\xi = \Delta/(1+c_\theta^2+c_\phi^2)^{\frac{1}{2}}$, $h_\theta = r$, $h_\phi = r \sin\theta$

$I$ = unit matrix

$J$ = total number of grid points in j-direction

$k_a$, $k_b$, $k_c$ = coefficients of thermal conductivity in the principal directions

$L$ = total number of grid points in l-direction

$\dot{m}_w$ = total rate of ablation ( summation of rates of ablation due to various reactions )

$N_i$, $N_j$, $N_m$ = shape functions

$n_j$, $n_{rc}$, $n_z$ = directional cosines of the normal to the boundary

$\bar{P}_i$ = load along the boundary

$q_{o,n}$ = heat flux transfered into the ablating wall

$q_{ra}$ = heat radiation of the air to the wall

$q_{w,\ smooth}$ = cold-wall heat flux on a smooth surface

$q_{rc}$, $q_z$ = heatfluxes in the radial direction and the axial direction

$q_\xi$, $q_\theta$, $q_\phi$ = heat fluxes in three directions of the transformed coordinate system

$\Delta Q_i$ = reaction heat per unit mass in the ith direction

$r$ = radial coordinate in the spheroidal coordinates

$r_c$ = radial coordinate in the cylindrical coordinates

$R_o$ = initial curvature radius at the nosetip

$r_i$, $r_j$ = radial coordinates of the boundary surface and the material surface in the spheroidal coordinate system

$s_p$, $s_u$ = load and displacement boundary

$t$ = time

$T$ = temperature

$u$ = displacement in radial direction

$u_i$ = displacement vector

$\bar{u}_i$ = known displacement vector

$v$ = axial displacement

$w$ = strain in the circumferential direction

$x$, $y$, $z$ = Cartesian coordinates

$\{\delta\}$ = column vector in which w and v of the nodal point are the parameters to be determined

$\Delta = r_j - r_i$ see Fig. 3

$\beta$ = half conic angle of the nosetip

$\varepsilon$ = radiation coefficient

$\theta$ = directional angle or the angle between the position vector and z-axis in the spheroidal coordinate system

$\xi$ = transformed coordinates

$\Pi$ = functional

$\rho$ = density

$\sigma$ = Boltzmann's constant

$\sigma_{ij}$ = stress tensor

$\sigma_r, \sigma_z, \sigma_\theta$ = radial stress, axial stress, and circumferential stress

$\phi$ = directional angle of the spheroidal coordinates

$\psi$ = heat blocking factor introduced by mass within the boundary layer

Subscripts

e = outer side of the boundary layer

j, l = nodal point numbers in $\xi$ and $\theta$, or z and r directions

o = initial conditions

w = wall

## 1. INTRODUCTION

It has long been a subject of interest to study and develop vehicle heat protection nosetips using carbon-base materials [1,3]. The most appealing advantages of the carbon-base nosetips are slight ablation and small shape changes. However, the thermal stress they experience under a shock heating environment is a problem of major concern. In order to investigate the nosetip heat protection, it is necessary to develop a computer code for a synthetic analysis algorithm to simultaneously calculate the thermal environment, ablation, heat transfer and thermal stresses. The present paper only gives examples for the plug-type nosetipe analysis, though the algorithm discussed here can also be applied for an analysis of shell-type nosetips.

For a heat protection nosetip, the state of the thermal stress depends not only on the mode of its structure, but also on the heat environment, ablation, the history of its shape changes and the instantaneous temperature fields in the body. Moreover, all these factors interfere with each other. Every effort has been made in recent studies to fully couple these factors in order to simulate realistic conditions as closely as possible.

## 2. ABLATION AND ABLATING CONTOUR

During re-entry, the thermochemical ablation of the heat protection layers of the carbon-base materials occurs mainly in an extremely high tmeperature range which is over 3000 °K. At such high temperatures, the thermochemical reactions occurring on the graphite surface can be considered as in a state of equilibrium [4]. During re-entry, the temperature on the surface of the heat protection layers increases quickly. At the beginning of the re-entry, there exists an influence of the non-equilibrium chemical reactions. Since the quantity of the ablative mass loss during this period is limited, it should not introduce appreciable errors when calculating the ablating processes during the whole re-entry

period under the assumption of chemical equilibrium.

Detailed analysis of the thermochemical ablation of the carbon-base nosetips, based on the JANAF thermodynamics data [6], and the screening calculations on the entire ablation surfaces along the trajectory for five carbon vapors and 10 carbon compounds, C (gas), $C_2$, $C_3$, $C_4$, $C_5$, CO, $CO_2$, $C_2O$, $C_3O_2$, CN, $CN_2$(C-N-N), $CN_2$(N-C-N), $C_2N$, $C_3N_2$, $C_4N_2$, whose thermodynamic data are available, are given in [5]. Results at the stagnation points are shown in Figure 1 where $f_c^{(i)}$ (i = 1,2,3,...,15) are the fractions of the ablated carbon in the total rate of thermochemical ablation in the chemical reactions to produce each gas or compound. Results show that on the ablation carbon surfaces, the chemical reactions producing CO, $C_3$, $C_2N$ and CN (corresponding to curves $f_c^{(6)}$, $f_c^{(3)}$, $f_c^{(13)}$ and $f_c^{(10)}$ in Figure 1) contributes more to the carbon ablation rate and/or to the thermal effects than to other effects. This makes the ablation calculations much simpler. Here, some of the secondary chemical reactions can be neglected during the calculations, and it is sufficient to take into account only the principal chemical reactions and corresponding chemical compositions, i.e.,

$$3C \rightleftharpoons C_3$$
$$C + \frac{1}{2}O_2 \rightleftharpoons CO \qquad (1')$$
$$C + \frac{1}{2}N_2 \rightleftharpoons CN$$
$$2C + \frac{1}{2}N_2 \rightleftharpoons C_2N_2$$

Thermodynamic data show that within the normal temperature range at the ablation surface, the equilibrium constants and the thermal effects of these reactions can be expressed nicely by the fitting formulas shown in Toble 1 and the approximate mean values. This makes the ablation calculations very convenient. The equilibrium constant of the carbon-oxygen reaction can be replaced by zero

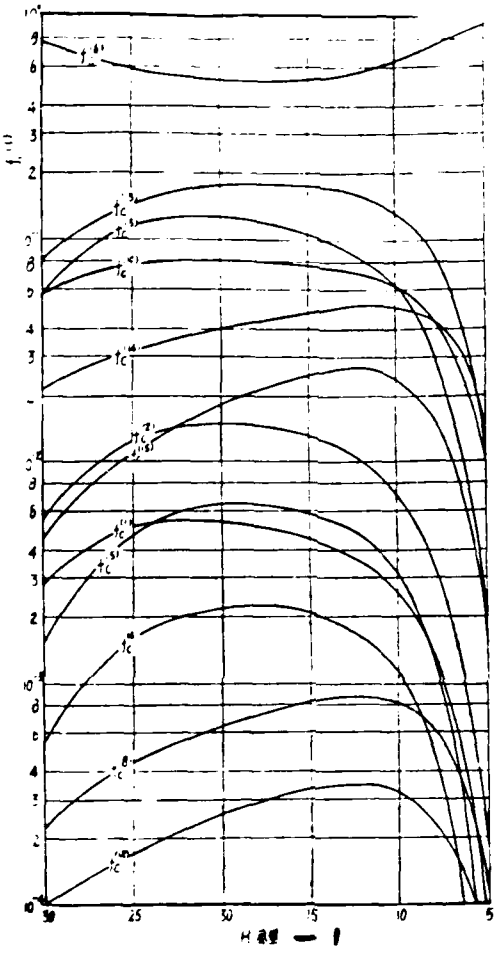

Fig. 1. Carbon ablation rate fraction changes in the reactions at the stagnant points on the wall along the trajectory. H - kilometer.

of the oxygen remainder. Based upon its equilibrium constant, the actual quantity of the oxygen remainder in this reaction is small enough to be negligible.

The thermochemical ablation rate of mass loss on the wall surfaces can be expressed as

$$m_w = B \cdot \psi q_{w_{\text{冷}}} / h_e \tag{1}$$

where the dimensionless rate of ablation, B,can be found through simultaneously solving the gas diffusivity equations in the boundary layer with the equilibrium constants of the chemical reactions.

The heat flux which gets into the burning wall is

$$q_{0,w} = \psi q_0 + q_{r_0} - \varepsilon \sigma T_w^4 \tag{2}$$

TABLE 1. The approximate equations of the equilibrium constants and thermal effects

| $\lg K_p = a - b \times 10^3 / T$ (°K) | | | $\Delta Q = c - d \times 10^{-3} T$ (°K) 千卡/克尔 | |
|---|---|---|---|---|
| 1 反 应 式 | a | b | c | d |
| $3C \rightleftharpoons C_3$ | 9.541 | 39.284 | 199.7 | 5.31 |
| $C + \frac{1}{2}O_2 \rightleftharpoons CO$ | | | −23.8 | 2.11 |
| $C + \frac{1}{2}N_2 \rightleftharpoons CN$ | 5.008 | 22.204 | 101.6 | 0 |
| $2C + \frac{1}{2}N_2 \rightleftharpoons C_2N$ | 6.572 | 28.448 | 137.6 | 1.98 |

1--chemical equation; 2--kcal/mole

where the second and third terms on the right of the equation are the radiation heat of the air to the wall and that of the wall to the air, respectively, and

$$q_e = q_{w,R}\left[\left(1-\frac{h_w}{h_e}\right)+\frac{B}{h_e}\sum_i f_i \Delta Q_i\right] \tag{3}$$

Provided that the mechanical peeling equations and those of the particle cloud erosion are given, their effect on the heat transfer, shape changes and thermal stresses, can be evaluated using the synthetic analysis computer code.

During the nosetip ablation, the equation describing the instantaneous contour changes is the following:

$$\frac{\partial r_j}{\partial t} = -\frac{\Delta}{h_t|_{r=r_j}}\cdot\frac{\dot{m}_w}{\rho} \tag{4}$$

where $m_w$ can be a summation of the mass losses caused by the ablation, peeling and erosion. This is a nonlinear hyperbolic type partial differential equation. The strategy to solve this equation is: first linearize the equation, then generate a difference equation which employs the implicit difference format and introduces artificial viscous terms and, finally, solve the difference equation using the iteration method. Details about these procedures can be found in [5] and [7]. Figure 4 which will be shown shortly gives the history of the contour changes of the heat protection nosetips evaluated using this algorithm at the same time when the temperature fields were calculated.

## 3. INSTANTANEOUS TEMPERATURE FIELDS

Since the carbon-base materials most likely exhibit an anisotropic behavior, it is necessary to calculate the heat transfer using the heat transfer equations for anisotropic materials as the starting point. When computing the instantaneous temperature fields for the plug-type nosetip structure, it seems better to divide the domain of interest into two parts, the main part and the plug handle of the nosetipe, between which an arbitrary boundary such as a spherical surface may be imagined. These two parts can be connected

artificially together as shown in Figure 2. For the main part, after a spheroidal coordinate system with corresponding origin of the coordinates is chosen and a moving coordinate system which is coordinated with the moving boundary is introduced, transformation between the two coordinate systems is given as

$$\xi = \frac{r - r_i}{\Delta(\theta, \phi, t)} \tag{5}$$

Consider the transformation of the moving burning boundary into a formal fixed boundary and the heat transfer equations involving three principal directions which are perpendicular to each other

$$\frac{\partial(\rho CT)}{\partial t} + \frac{\partial}{\partial x}\left(k_a \frac{\partial T}{\partial x}\right) + \frac{\partial}{\partial y}\left(k_b \frac{\partial T}{\partial y}\right) + \frac{\partial}{\partial z}\left(k_c \frac{\partial T}{\partial z}\right) = 0 \tag{6}$$

into

$$\frac{\partial(\rho CT)}{\partial t} - \frac{\xi}{\Delta}\frac{\partial \Delta}{\partial t}\frac{\partial(\rho CT)}{\partial \xi}$$

$$= -\left[\frac{1}{r^2}\frac{\partial}{\partial \xi}\left(\frac{r^2}{h_t} q_t\right) + \frac{1}{h_\theta \sin\theta}\frac{\partial}{\partial \theta}(r\Delta \sin\theta\, q_\theta) + \frac{1}{h_\phi r \Delta}\frac{\partial}{\partial \phi}(r\Delta q_\phi)\right.$$

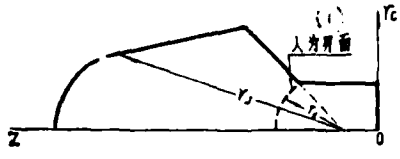


Figure 2. The coordinate system
1--artificial boundary

where the $\partial\Delta/\partial t$ is the rate of thickness, i.e., the rate of contour changes, $\partial r_s/\partial t$ in equation (4). The conditions for heat transfer along the burning boundary are

$$\xi = 1, \qquad q_t = -Q \tag{8}$$

where

$$Q = q_{e,a} + \rho\left(\int_{T_a}^{T_w} C\,dT\right)(1 + C_\theta^2 + C_\phi^2)^{-\frac{1}{2}}\frac{\partial \Delta}{\partial t} \tag{9}$$

Only bodies with rotational symmetry at zero angle of attack and having isotropic behavior (at least within the plane perpendicular to the wind axis, i.e., $k_a = k_b$) have derivative terms involving $\phi$ cancel. Then the problem is simplified to an axisymmetric one. For the transformed equation (7) as for an

axisymmetric problem, the first and second derivatives of temperature with respect to the space coordinate and the derivatives of heat flux with respect to space coordinates within the domain all assume a central difference form with the second order of accuracy. Along the boundary, either the central difference or the forward or backward difference with the second order of accuracy is assumed. The derivatives of temperature with respect to time take on the DuFort-Frankel difference form. Then in the difference equation within the domain, it is assumed that

$$T^n_{i,j} = \frac{1}{2}(T^{n+1}_{i,j} + T^{n-1}_{i,j}) + 0(\Delta t^2) \tag{10}$$

where the superscripts such as n, denote the numbers of time steps. Neglecting the higher order terms and rearranging this equation, one obtains a three-level explicit difference equation, which is suitable for computation with good stability. Reference [5] gives the details about the derivation of this equation. An example of an exact analytic solution using this algorithm is also given with satisfactory accuracy and there is not much influence of the time steps on the computation.

Since there is no moving boundary for the plug-handle part, it is better to use a fixed cylindrical coordinate system. For rotational bodies at zero angle of attack and $k_a = k_b$, the heat transfer equation can be written in the following axisymmetric form:

$$\frac{\partial(\rho CT)}{\partial t} = \frac{1}{r_*}\frac{\partial}{\partial r_*}\left(r_* k_* \frac{\partial T}{\partial r_*}\right) + \frac{\partial}{\partial z}\left(k_* \frac{\partial T}{\partial z}\right) \tag{11}$$

When connecting the major part and the plug-handle, one must consider the conditions of heat flux continuity along the artificial boundary between them.

Attention should be paid to the following facts when solving equation (11) numerically using the difference method: for the $\theta$-coordinate in the spheroidal coordinate system, the major part is divided into a uniform grid network. However, the distribution of the grid points located on the boundary is not uniform corresponding

to $r_c$ direction in the cylindrical coordinate system. To establish the connection conditions of the normal heat flux continuity at both sides of the boundary, it is required that the grid points falling onto the boundary surface by the grid network within the plug-handle part coincide with those of the main part. This makes it necessary to divide the plug-handle part into a non-uniform grid network to meet this requirement. In addition, the boundary is also irregular. To harmonize such a distribution with that of the main part, it is necessary to develop a three-level explicit difference algorithm for this non-uniform grid network. Specifically, for the in-domain points, Taylor series expansion can be applied to the domain using the temperatures or heat fluxes at their neighboring points to obtain the difference approximation to the temperature or heat flux derivatives at those points with unequal steps. For example:

$$\left(\frac{\partial T}{\partial r_e}\right)_{j,l} = \frac{1}{\Delta r_{ej,l}+\Delta r_{ej,l+1}}\left[\frac{\Delta r_{ej,l}}{\Delta r_{ej,l+1}}T_{j,l+1}+\left(\frac{\Delta r_{ej,l+1}}{\Delta r_{ej,l}}-\frac{\Delta r_{ej,l}}{\Delta r_{ej,l+1}}\right)T_{j,l}\right.$$

$$\left.-\frac{\Delta r_{ej,l+1}}{\Delta r_{ej,l}}T_{j,l+1}\right]+0(\Delta r_{ej,l}\cdot\Delta r_{ej,l+1}) \tag{12}$$

$$\left[\frac{\partial}{\partial z}\left(k_e\frac{\partial T}{\partial z}\right)\right]_{j,l} = \frac{1}{\frac{1}{2}(\Delta z_{j,l}+\Delta z_{j+1,l})}\left\{\left(\frac{\Delta z_{j,l}}{\Delta z^2_{j+1,l}}k_{ej+\frac{1}{2},l}\right.\right.$$

$$+\frac{\Delta z_{j+1,l}-\Delta z_{j,l}}{\Delta z^2_{j+1,l}}k_{ej,l}\Big)T_{j+1,l}+\left(\frac{\Delta z_{j+1,l}}{\Delta z^2_{j,l}}k_{ej-\frac{1}{2},l}+\frac{\Delta z_{j,l}-\Delta z_{j+1,l}}{\Delta z^2_{j,l}}k_{ej,l}\right)T_{j-1,l}$$

$$-\left[\frac{\Delta z_{j,l}}{\Delta z^2_{j+1,l}}k_{ej+\frac{1}{2},l}+\frac{\Delta z_{j+1,l}}{\Delta z^2_{j,l}}k_{ej-\frac{1}{2},l}-\left(\frac{1}{\Delta z_{j,l}}-\frac{1}{\Delta z_{j+1,l}}\right)^2(\Delta z_{j,l}\right. \tag{13}$$

where $\left.\left.+\Delta z_{j+1,l})\,k_{ej,l}\right]T_{j,l}\right\}+0\left(\frac{\Delta z_{j,l}\cdot\Delta z_{j+1,l}}{\Delta z_{j,l}+\Delta z_{j+1,l}}\right)$

$$\begin{cases}\Delta r_{ej,l}=r_{ej,l}-r_{ej,l-1}\\ \Delta z_{j,l}=z_{j,l}-z_{j-1,l}\end{cases} \tag{14}$$

With the same technique used in the main part, the three-level explicit difference equations for the non-uniform mesh can be developed.

The boundary condition for the irregular boundary is

$$k_e\frac{\partial T}{\partial r_e}n_{re}+k_e\frac{\partial T}{\partial z}n_e=f(T,r_e,z,t) \tag{15}$$

Since the grid lines are not necessarily parallel to the boundary lines, the structure of the difference format is more complicated. For the boundary mesh shown in Figure 3, in order to derive the unequal step difference expressions to the first order derivatives of the temperatures at boundary nodal point, (J, 1) with the second order of accuracy, the difference expressions for the second order derivatives which include the cross terms must be derived simultaneously so as to generate the difference equations for boundary condition equation (15). When the partial derivatives are approximated by the non-uniform difference, there is no need to make any artificial assumptions usually made at the boundary, except that the difference is used to approximate the derivatives. As a result, a more satisfactory solution can be obtained.

What has been mentioned above has been realized in our synthetic analysis program. Calculations show that, similar to the uniform difference format, the time step in the non-uniform case does not have much influence on the accuracy and stability of solutions under the sample calculation conditions.

Results of the sample calculations for the history of the graphite plug-type nosetip ablation and heat transfer during re-entry are shown in Figure 4.

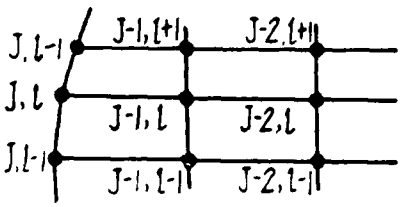


Figure 3. The mesh around nodal point (J, 1).

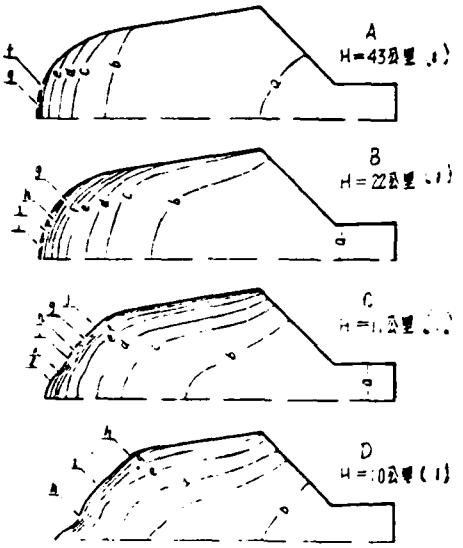


Figure 4. Temperature fields and ablation contour of the plug-type carbon-base nosetip at different altitudes during re-entry.
1--km.

## 4. STRESS AND STRAIN FIELDS

Since the carbon-base materials have a very small range of plasticity, the objects of this study are limited to those of linear elasticity with small strains. To calculate thermal stress fields and thermal strain fields from the known temperature distribution, the incomplete generalized potential energy principles [8] are used, i.e., the small displacement linear elasticity principles which take into account the boundary load and the boundary displacement conditions and only satisfy the strain-displacement relationship,

$$\Pi = \iiint_{v} [A(e_{ij}) - F_i u_i] dv - \iint_{S_p} \bar{P} u_i ds - \iint_{S_u} (u_i - \bar{u}_i) \sigma_{ij} n_j ds \tag{16}$$

with the finite element method. Note that the subscripts i and j in the equation denote the corresponding components and the summation operation. The axisymmetric problems can be simplified into those within the meridian plane in the cylindrical coordinate system. Triangles are selected as the finite elements, and in order to avoid the curious integral along the symmetric axis, reference [9] suggests that, except that the parameters to be determined at the nodal points include the axial displacement, v, the circumference strain is directly assumed as

$$w = \frac{u}{r_e} \tag{17}$$

A linear interpolating function can be constructed in an element by these unknown parameters.

$$\begin{Bmatrix} w \\ v \end{Bmatrix}^e = [IN_i \; IN_j \; IN_m] \{\delta\}^e \tag{18}$$

where superscript, e, indicates the value in an element and $\{\delta\}^e$ is the unknown nodal point parameter column matrix in the element.

$$\{\delta\}^e = [w_i \; v_i \; w_j \; v_j \; w_m \; v_m]^{eT} \tag{19}$$

Use interpolating function (18) to calculate the integral in equation (16), find the summation for all elements to compose the general functional. Then get the stationary values, i.e., a set of linear equations which contain a symmetric coefficient matrix in which v and w are unknowns. Then find the nodal point parameters to be determined. The order of this matrix is twice the total amount of nodal points. Accordingly, the strain and stresses can be solved based upon the relationships between strain and displacement and stress and strain.

In equation (16), the boundary conditions are entirely brought into the functional. This not only makes the scheme dealing with the boundary conditions more reasonable, but also helps investigate the influence of various types of boundary conditions. An urgent problem which needs to be solved is that only the outside boundary which is subjected to aerodynamic pressures has been dealt with so far, while the more important contact surfaces have not been studied yet, or only treated as a free boundary. In

order to fully investigate such boundary conditions, the author divides the boundary conditions into three categories, then gives the derivation and sample computation. The first category is of free boundary; in the second category, displacement on the boundary is assigned in advance, e.g., a zero boundary displacement; and in the third one, the boundary displacement is partially assigned, such as the case where only the tangential displacement is allowed, but not allowed in the normal direction. It undoubtedly deals with the mixed boundary conditions involving simultaneously the three types of boundaries with more ease.

## 5. NUMERICAL METHOD FOR SHAPE-SELECTING

It seems very clumsy to generate in advance each finite element grid when computing the thermal stresses for the nosetips with different original contours. Even for the nosetips with the same original contour, the contour changes with time due to the ablation. It is, therefore, almost impossible to generate each grid network manually for the nosetips with their instantaneous contours. Thus, thermal stresses can usually be estimated only from a fixed contour or a few contour changes. Moreover, each time one calculates a shape, one has to generate one grid system. So it is necessary to develop a special technique which can be used to generate automatically the finite element grid network as the shape of the body changes. The author developed such an automatic grid generation technique in editing this synthetic analysis computer code. The finite element grid mesh generated by this technique not only can automatically match the changing shapes caused by the ablation, but also can automatically match various original contours with different dimensions, provided that the adjustable dimensions of the original shapes are available. As shown in Figure 5, after the adjustable parameters $R_o$, $z_c$, $z_B$, $\beta$ and $\theta_L$ are properly selected, the finite element can be computed for various bodies with the required shapes. The shape-selection computation can be easily performed after selecting the different combinations of these adjustable parameters. Furthermore, combining the

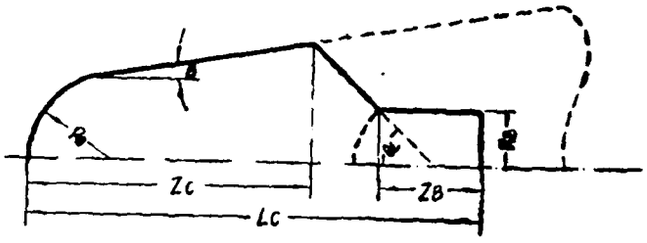


Fig. 5. The adjustable parameters of the initial contour of the plug-type nosetips

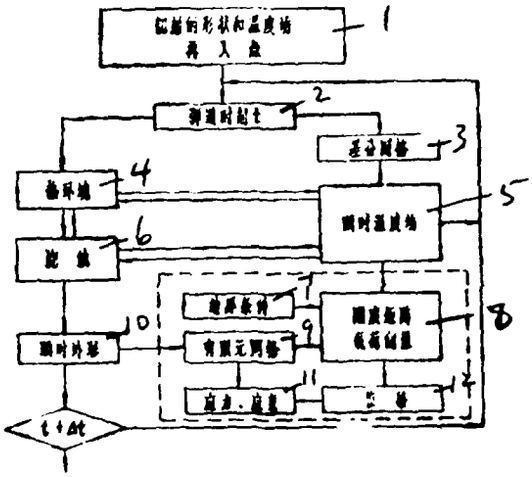

Fig. 6. Flow chart of the compute code

1- Original contour and temperature field at the re-entry point; 2- Trajectory time, t; 3- Difference mesh; 4- Thermal environment; 5- Instantaneous temperature field; 6- Ablation; 7- Boundary conditions; 8- Rigidity matrix and load vector; 9- Finite element mesh; 10- Instantaneous contour; 11- Stress and strain; 12- Displacement.

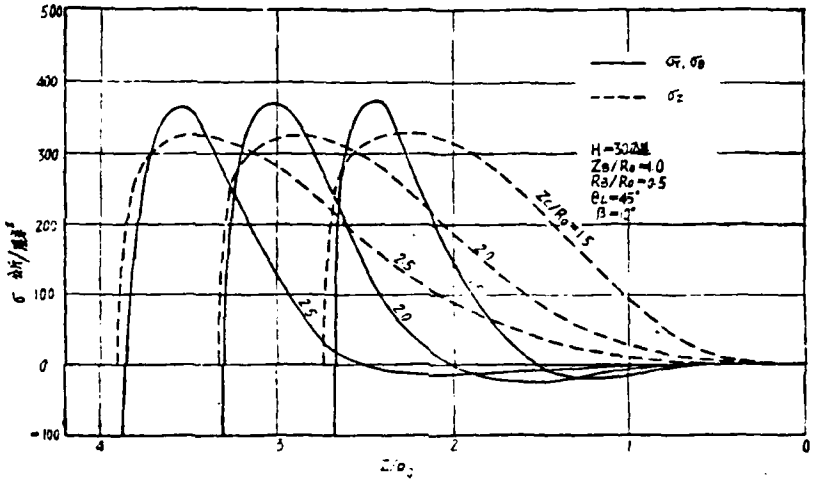


Fig. 7. Influence of the axial extent length on the stress distribution .

quantitative analysis of the effects of different boundary conditions, it is possible to provide a useful basis for the engineering designs.

The synthetic analysis computer code edited starts the calculations from the re-entry point, then for the thermal environment, based on the trajectory and body parameters, followed by the estimation of the ablation and instantaneous temperature fields. The calculations for the thermal environment, ablation and instantaneous temperature fields are coupled. The code computes the instantaneous contours, based on the ablation calculation results; from the instantaneous contour and instantaneous temperature fields and considering various types of boundary conditions, the code calculates the stress fields and the strain fields at that instant. The difference grid mesh and the finite element grid mesh, changing with the instantaneous contours, are automatically generated at every instant. A brief flow chart of the complete computer code is shown in Figure 6.

Since the time step can be taken as long as 0.2 second when computing the temperatures and the contours, the time spent during computing all these parameters along a trajectory is limited.

As an example, results of the selecting calculations of the graphite nosetips for one of the parameters $z_c$ are shown in Figure 7.

## 6. CONCLUSIONS

A synthetic analysis algorithm in which the thermal environment, ablation, heat transfer and thermal stresses are considered and an automatic grid generation technique has been developed, is briefly introduced. With this synthetic analysis computer code, it is possible to perform a comprehensive numerical analysis for ablation, heat transfer and thermal stresses during re-entry of the carbon-base nosetips into the atmosphere. Calculations were made for nosetip shapes and the connection format of their contact surfaces.

## REFERENCES


[ 1 ] Segletes John A.: J. of Spacecraft & Rockets, 12, 1975.
[ 2 ] Chin, Jin H.: AIAAJ, 13, 1975, 5.
[ 3 ] Schneider, P. J., Teter, R. D., Coleman, W. D., Heath, R. M.: J. of Spacecraft & Rockets, 10, 1973, 9.
[ 4 ] Lundell, J. H., Dickey, R. R.: AIAAJ, 11, 1973, 2.
5. Huang, Zhen-zhong, Acta Aerodynamica Sinica, January 1981.
[ 6 ] JANAF Thermochemical Tables, 2nd edi., NSRDS-NBS37, 1976.
[ 7 ] Cromwell, P. G.: SAMSO-TR-76-8.
8. Qian, Wei-chang, Mechanics and Practices, January 1979.
9. Qian, Wei-chang, Applied Mathematics and Mechanics, January 1980.



**Abstract**

In this paper, the principle of synthetic analysis calculation and some treatment technics about reentry thermal environment, ablation, conduction and thermal stresses of vehicles are described briefly. The thermochemical ablation calculation for chemical reactions on the ablating surface of carbonbase materials. is simplified by using selective calculation result. The temperature fields are calculated by means of the three level explicit difference schemes for both constant and unconstant space steps within total region. The thermostresses are calculated by the finite element method, which is based on the noncomplete generalized potential energy variational principles under the supposed condition of linear elasticity. The calculation method of the effects for various displacement boundary condition are provided. An automatic mesh dividing technic is realized in the comprehensive analysis procedure and selective calculations for shapes can be made with this technic conveniently.

END

FILMED

5-86

DTIC